Bulletin of the Geological Society of Malaysia, No. 66, December 2018, pp. 15 – 23

Complex geothermal gradients and their implications, deepwater Sabah, Malaysia

Steve McGiveron[1,*] & John Jong[2]

[1] Independent Marine Geoscience Consultant, UK
[2] JX Nippon Oil and Gas Exploration (Deepwater Sabah) Limited
* Corresponding author email address: smcgiveron@outlook.com

Abstract: Seabed heat flow measurements together with values estimated from the position of the base of the gas hydrate stability zone mapped from 3D seismic data from a deepwater study area in Block X approximately 100 km offshore Sabah, Malaysia, are discussed. The data show a variable and high geothermal gradient that is consistent with the regional trend of 6-9°C/100m. Rising plumes of warm fluid and locally remobilised mud are abundant and are interpreted to be responsible for the high values, locally creating zones of very high gradients in excess of 20°C/100m above the plumes. In contrast, initial interpretation of data from the Block X exploration wells show geothermal gradients greater than the regional average (5.08 to 5.66°C/100m compared to 4.43°C/100m) but still significantly lower than the shallow values. Reinterpretation of the deep geothermal gradient well data suggests that the regional gradient fits these data if the influence of the warm fluid plumes on the shallow section is taken into account. The resultant gradient is no longer a simple linear function but a complex curve that varies depending upon the offset of a well from the areas of anomalous warming in the shallow section. A lower geothermal gradient at reservoir depth, as suggested by this study, could have important implications for hydrocarbon maturation and generation, as well as for equipment selection for well operations.

Keywords: Deepwater Sabah, geothermal gradients, heat flow

INTRODUCTION

Heat flow and geothermal gradients in the South China Sea offshore of Borneo, Malaysia, have long been studied on a regional scale by commercial oil and gas companies and academia researchers (e.g., Hall & Morley, 2004). However, in detail, the deepwater seabed is not uniform but displays many features indicative of active fluid flow including seeps and mud volcanoes (van Rensbergen & Morley, 2001; Zielinski *et al*., 2007; McGiveron & Jong, 2016).

The objective of this paper is to describe detailed heat flow observations within a deepwater study area approximately 100 km offshore on the lower continental rise of the NW Borneo Fold thrust Belt (Block X Study Area, Figures 1 and 2). Here the seabed and shallow geological section is disturbed by fluid flow from depth that influences the local geothermal gradient. A model with a complex composite geothermal gradient is presented to integrate the shallow observations with the apparently conflicting deeper results from wells. The implications of the model are also discussed.

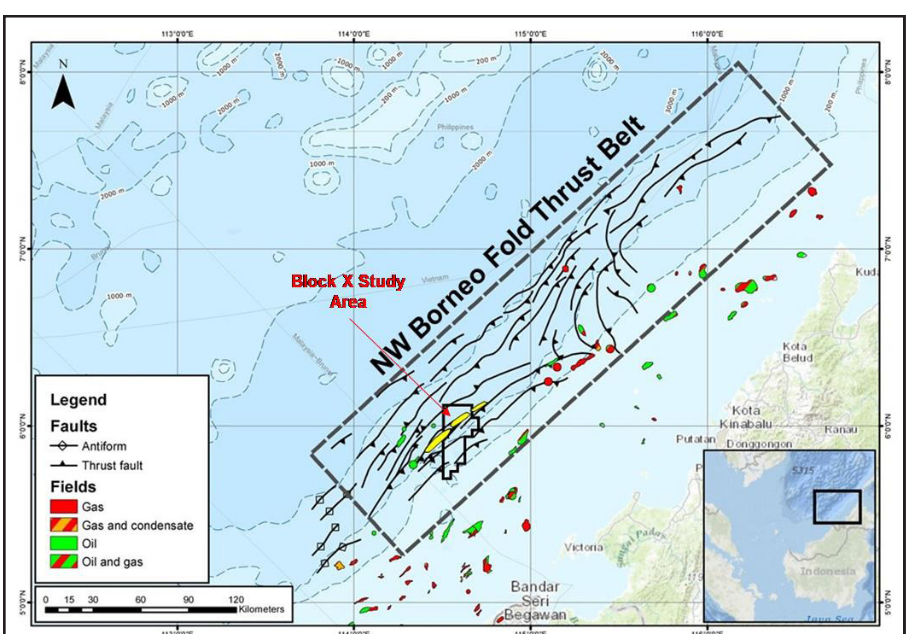

Figure 1: Location map of offshore deepwater Sabah Block X (solid black polygon) within the NW Borneo Fold Thrust Belt (from Ogawa & Jong, 2016).

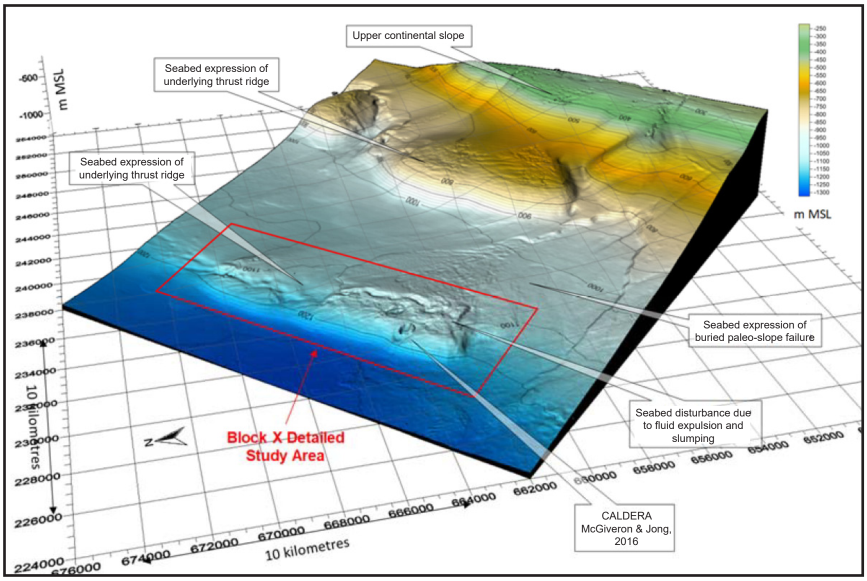

Figure 2: Three dimensional image of the seabed illustrating the geomorphological setting of the Block X Study Area.

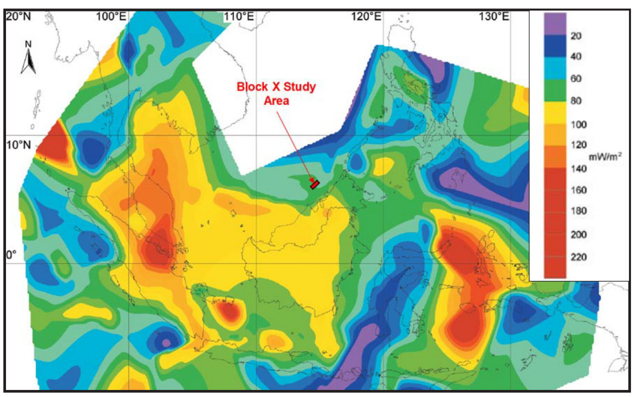

Figure 3: Contoured heat flow map for SE Asia (Hall & Morley, 2004) based on the database of Pollack *et al*. (1990, 1993) and oil company compilations by Kenyon & Beddoes (1977), and Rutherford & Qureshi (1981).

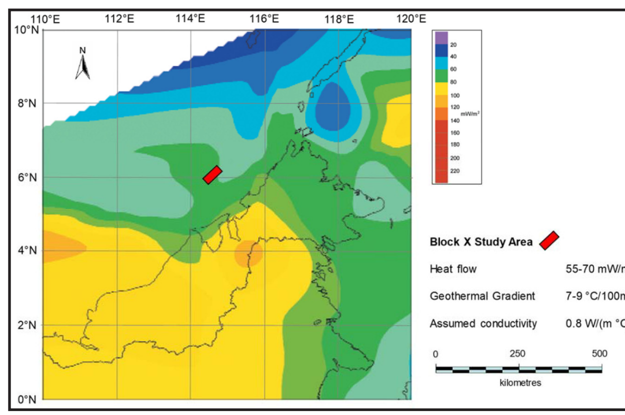

Figure 4: Contoured heat flow map detail for NW Borneo expanded from Hall & Morley (2004).

REGIONAL HEAT FLOW SETTING

The regional heat flow within the South China Sea and the deepwater basins offshore of Borneo has been studied by several authors. Hall & Morley (2004) presents a contoured compilation of heat flow data derived from the database of Pollack *et al*. (1990, 1993) and oil company compilations by Kenyon & Beddoes (1977) and Rutherford & Qureshi (1981). It is reproduced here as Figure 3. Heat flows are very variable reflecting the complex nature of the area.

The regional contoured heat flow map detail for NW Borneo expanded from Hall & Morley (2004), including deepwater Block X Study Area, is illustrated on Figure 4. The regional heat flow varies between a low of less than 40 mW/m^2 (5°C/100m) north of 8°N and 80-120 mW/m^2 (10-15°C/100m) south of 5°N and west of 117°E. At deepwater Block X Study Area, the estimated heat flow range from these data is 55-70 mW/m^2 (7-9°C/100m) (Jong *et al*., 2013; Figure 5). Similar values of between 55-75 mW/m^2 (6.9-9.4°C/100m) are presented by Hall (2002).

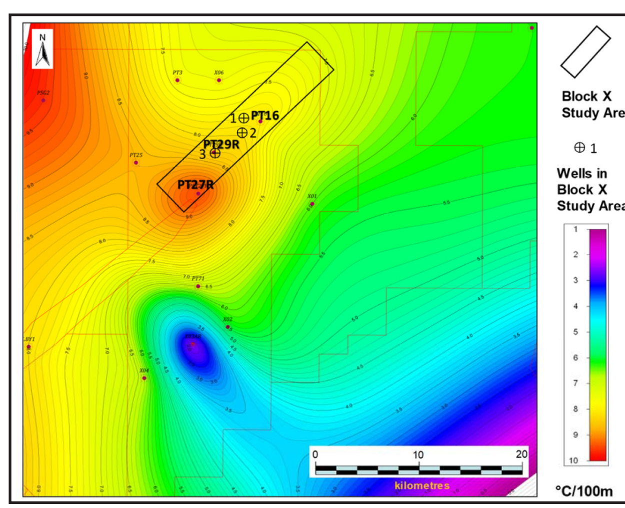

Figure 5: Regional geothermal gradient map based on JX Nippon seabed heat flow data contoured by Jong *et al*. (2013) in °C/100m.

Regional heat flow data to the south-west from 186 sites on the Brunei margin, reported by Zielinski *et al*. (2007), are also comparable, varying between a mean of 59.0 mW/m^2

(7.4°C/100m) in the deepwater basins and a mean of 83.7 mW/m^2 (10.5°C/100m) on the landward margin.

BLOCK X SEABED HEAT FLOW

Seabed heat flow measurements were carried in 2013 by JX Nippon Oil & Gas Exploration (Deepwater Sabah) Limited both within and in the vicinity of the Block X Study Area (Searie, 2013). Data were recorded using miniaturised data loggers (MTLs) mounted on the outside of corer barrels. A total of 21 stations were occupied; 8 stations with a 3 m corer barrel and 13 stations with a 2 m corer barrel. The MTLs were spaced at 50 cm intervals on the 3 m corer barrels. However, after damage was incurred on the ninth station, the corer barrel length was reduced to 2 m and the six MTLs were spaced at 33 cm intervals.

The transient effects of bottom water temperature variations influenced the shallowest 6 sampling stations and appropriate corrections were applied. The deepwater data however were not subjected to significant transient effects and no corrections were applied.

The deepwater stations of interest to the present discussion from greater than 1000 m water depth are presented in Table 1.

The data results from the heat flow stations were upscaled from °C/m to °C/100m to maintain consistency of scale with Jong *et al*. (2013). Noted several other authors have quoted gradients at the greater scale of °C/1000m (Anonymous JOIDES, 1992; Shankar *et al*., 2004; Laird & Morley, 2011; Minshull, 2011). It is acknowledged that upscaling, although theoretically justified, is a potential source of error and can be misleading. However, the robustness of upscaling of these data from metre scale to 100 metre scale is supported by:

- Similarity with heat flow gradients determined from the depth of the base of the gas hydrate stability zone at between typically 120 m and 140 m below seabed.
- Seabed Station PT29R lying only 60 m north-west of Well 3 records the same geothermal gradient as that determined by calculation from the observed base of the gas hydrate stability zone in the well.

The full data set was initially analysed by Jong *et al.* (2013), and their geothermal gradient map scaled in °C/100m is presented here as Figure 5. The geothermal gradients increase from a low of around 3°C/100m in the south-east to a high of approximately 10°C/100m in the north-west.

The contoured geothermal gradient within the Block X Study Area increases from 7°C/100m in the north-east to 9°C/100m in the south-west where an anomalous contour "bulls eye" is present. These values are consistent with the regional results for the deepwater basins presented by Hall & Morley (2004) and Zielinski *et al*. (2007).

Apparently anomalous high and low values in the central west creating "bulls eye" contours around the sampling stations were initially dismissed as false and a product of the sampling distribution. However, detailed mapping with the Block X Study Area supports a geological origin for the anomalously high value. The anomalously low value lies beyond the study area and is not considered further herein.

GEOTHERMAL GRADIENT DERIVED FROM GAS HYDRATE STABILITY

The base of the methane gas hydrate stability zone is a phase boundary. In its simplest setting for pure methane, which constitutes over 99 % of the hydrocarbon gas mixture (Kvenvolden, 2000), the phase boundary is a function of pressure (depth) and temperature (geothermal gradient). The phase boundary is commonly visible in deepwater seismic data as a bottom simulating reflector (BSR) that can be mapped using standard seismic techniques, as investigated by Goh *et al*. (2017) in the study area.

Fluid flow through the sub-seabed sediments, often focused within anticlines, increases the geothermal gradient, raising the temperature at the base of the gas hydrate stability zone and shallowing its depth below seabed as illustrated in Figure 6 (Laird & Morley, 2011). The changes in the sub-seabed depth of the BSR can therefore be used to estimate the variations in heat flow and geothermal gradient (Grevemeyer & Villinger, 2001; Shankar *et al.*, 2004; Lopez & Ojeda, 2006; Minshull, 2011).

Table 1: Deepwater (>1000m) geothermal gradient and heat flow stations in Block X.

Station	Latitude degrees	Longitude degrees	Water Depth m	mean k W/(m°C)	Gradient dT/dZ °C/m	Heat Flow q mW/m^2	Core barrel length (m)	Comments
PT16	6.02009	114.61511	1116	0.790	0.078	61.6	2	Study Area
PT3	6.05591	114.54272	1343	0.781	0.074	58.5	2	
PT25	5.98345	114.50694	1270	0.821	0.086	71.5	2	
X06	6.05609	114.57883	1325	0.794	0.073	58.7	2	
PT29R	5.99281	114.57463	1107	0.810	0.082	65.3	2	Study Area
PPT27R	5.95652	114.56124	1117	0.783	0.094	72.7	2	Study Area
		AVERAGE	*1213*	*0.797*	*0.081*	*64.7*		
		AVERAGE for Block X Study Area	*1113*	*0.794*	*0.085*	*66.5*		

The bottom simulating reflector within the Block X Study Area was interpreted from the exploration 3D seismic data as a discontinuous phase reversal event. The geothermal gradient was subsequently back calculated using the JOIDES (1992) formula using the calibrated seabed and BSR depths and the average value of conductivity for the Block X Study Area derived from the JX Nippon seafloor heat flow survey presented in Table 1. Locally where the gas hydrate stability zone is thin and difficult to map (typically less than 20 m) the calculations are considered unreliable and as a result the maximum value has been clipped at 20°C/100m. A comparison between the BSR derived geothermal gradients and those observed at the three seabed sampling stations (Searie, 2013) and in the tophole of three exploration wells within the Block X Study Area is presented in Table 2. The differences generally are within ±6 % with a maximum observed difference of 12 %. Seabed Station PT29R lies only 60 m north-west of Well 3 and both record the same geothermal gradient.

The geothermal gradients derived from the mapped BSR in the Block X Study Area were overlain on the regional geothermal map (Jong *et al*., 2013) and displayed at the same scale (Figures 7 and 8). There is a general good correlation between the gradients derived by the two methods. Several clusters of higher geothermal gradients

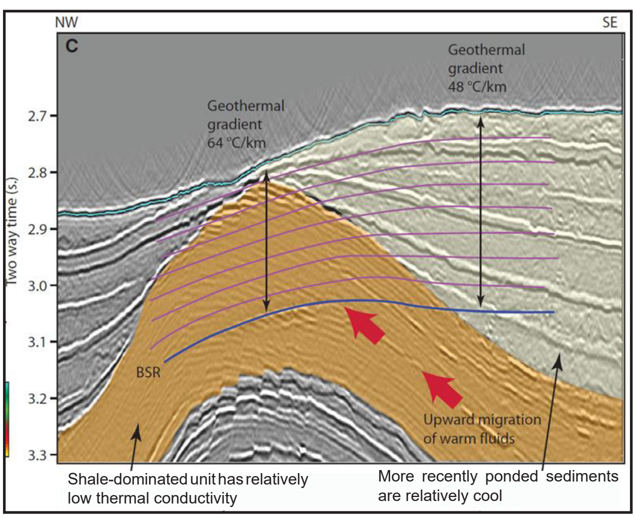

Figure 6: Geothermal Gradient variations across an anticline, deepwater Brunei, due to migrating fluid (Laird & Morley, 2011).

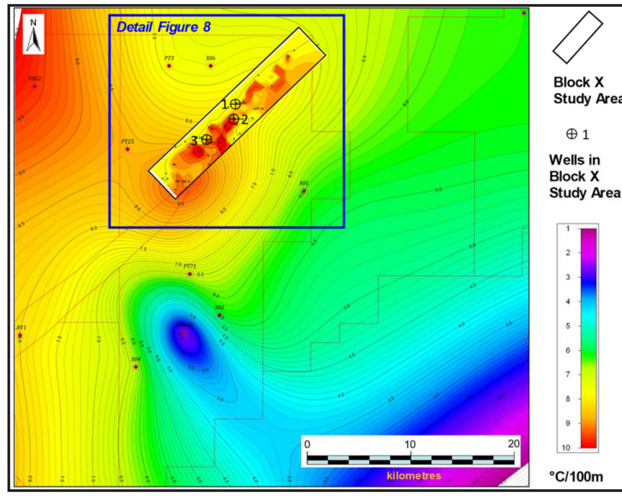

Figure 7: BSR derived geothermal gradients overlain on regional geothermal gradient map (Jong *et al*., 2013).

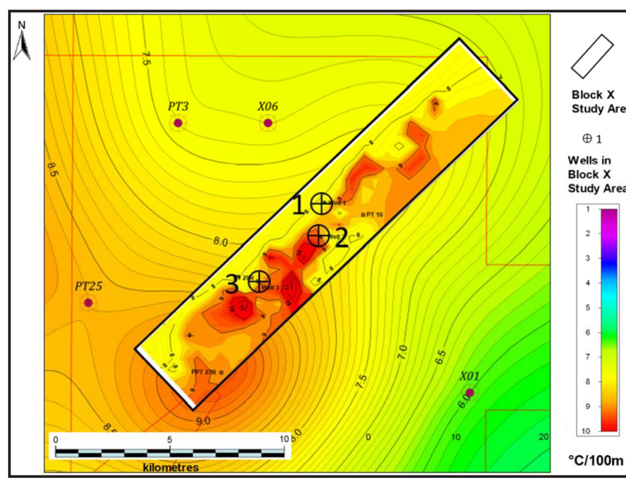

Figure 8: Detail BSR derived geothermal gradients overlain on regional geothermal gradient map (Jong *et al*., 2013).

Table 2: Comparison between observed and BSR calculated geothermal gradients.

Type	Reference	Gradient dT/dZ °C/m Observed 2m corer	Gradient dT/dZ °C/100m	Gradient dT/dZ °C/100m from mapped BSR	Difference % mapped-observed
Seabed Station (Searie, 2013)	PT16	0.078	7.8 (upscaled)	8.7	12
Seabed Station (Searie, 2013)	PT29R	0.082	8.2 (upscaled)	8.6	5
Seabed Station (Searie, 2013)	PPT27R	0.094	9.4 (upscaled)	8.9	-5
Exploration well (from logged hydrate)	1		7.7	8.2	6
Exploration well (from logged hydrate)	2		8.6	9.6	12
Exploration well (from logged hydrate)	3		8.2	8.7	6
	Average		*8.3*	*8.8*	*5.9*

are however identified by the more detailed BSR method particularly in the south-west of the Block X Study Area and may be the reason for the higher than average values recorded in seabed station PPT27R that resulted in the contour "bulls eye" on the regional map.

In detail the distribution of the shallow geothermal gradients derived from the mapped gas hydrate BSR is complex (Figure 9). In the central south-west the highest gradients are related to fluid flow plumes and a mud volcano caldera (McGiveron & Jong, 2016), as illustrated on Figure 10. Geothermal gradients within the plumes are estimated to be in excess of 20°C/100m, the effective limit of resolution of the method in this area. True gradients may be much higher as Zielinski *et al*. (2007) reported that on the adjacent Brunei margin a single megaseep has exhibited a maximum heat flow of 604 mW/m^2 (approximately 75°C/100m).

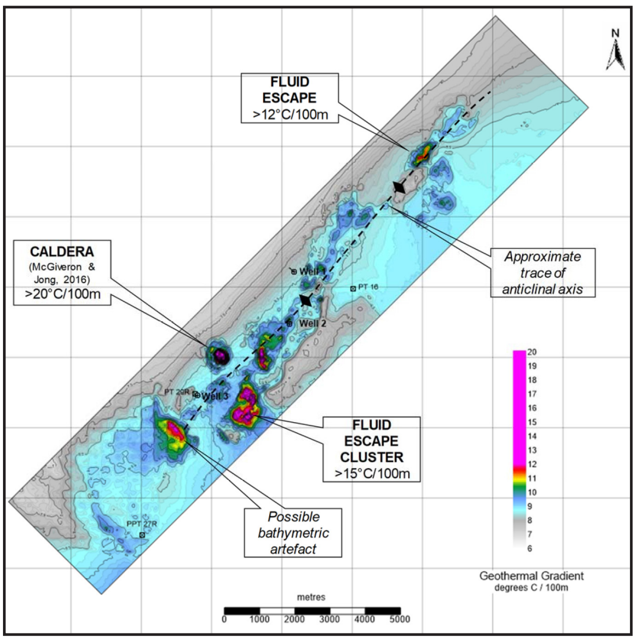

Figure 9: Geothermal Gradient variations within the Block X Study Area derived from the mapped BSR.

In the north-east an isolated area of high geothermal gradient is related to a single fluid escape pipe originating from the deep anticlinal crest and passing through a shallow dispersive fan (Figure 11). The estimated geothermal gradient is 12°C/100m within the fluid escape, approximately 4°C/100m greater than the host sediments.

GEOTHERMAL GRADIENTS FROM WELL DATA

The regional geothermal gradient derived from deep measurements from four wells offshore Sabah display a geothermal gradient trend of 4.43°C/100m (Figure 12). The Block X well data appear to display a higher gradient than the regional trend when fitted to a simple linear function passing through the temperature-depth origin. Within the Block X Study Area, the average gradient for Well-1 and Well-2 is 5.08°C/100m, whilst the Well-3 gives a geothermal gradient of 5.66°C/100m (Figure 13).

It is noteworthy that all the deep data show a significantly lower gradient compared to the seabed geothermal gradient measurements and the calculations in the shallow section derived from the base of the gas hydrate stability zone.

It is suggested here that these apparently conflicting data can be resolved if the influence of heat input into the shallow section from rising fluid and mobilised mud is taken into account.

INTEGRATED GEOTHERMAL GRADIENT MODEL

Figure 14 illustrates the typical linear shallow geothermal gradient (in brown) derived from the depth of

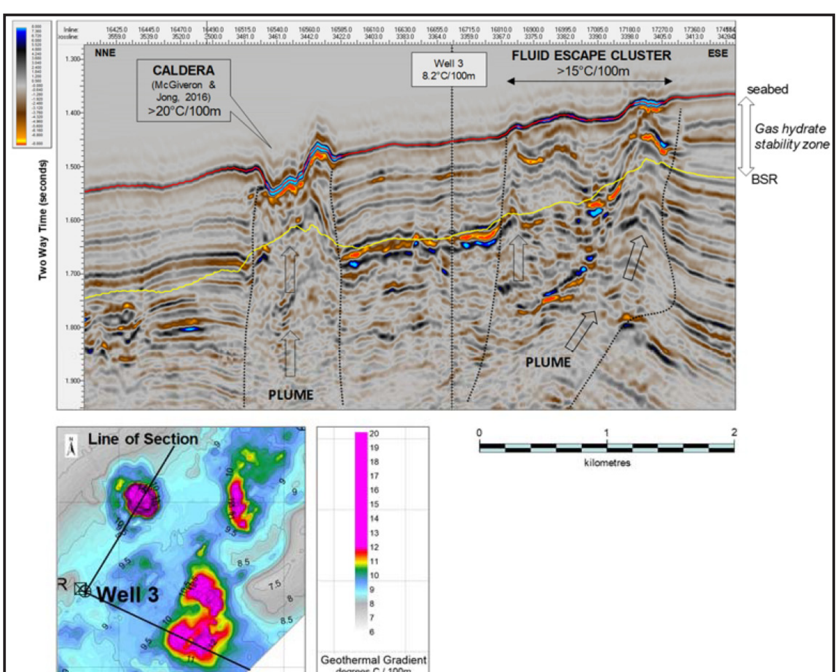

Figure 10: High geothermal gradients associated with fluid plumes rising from depth and mud mobilisation within caldera.

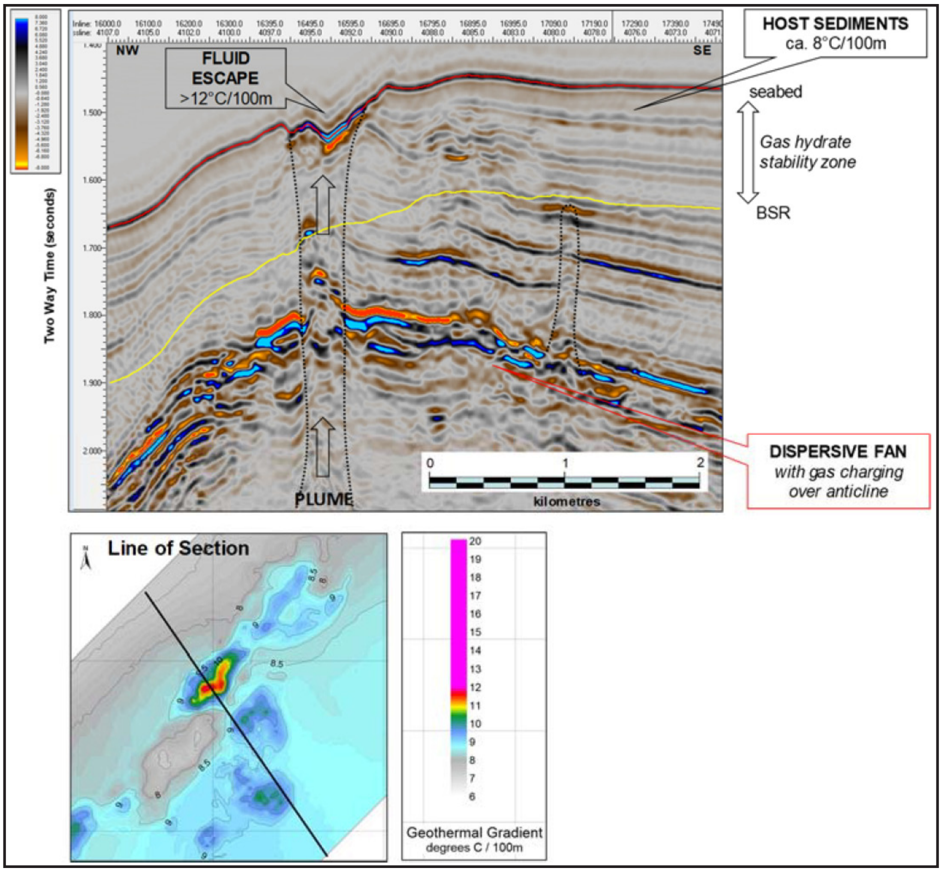

Figure 11: High geothermal gradients associated with fluid plume rising from depth passing through fan deposit.

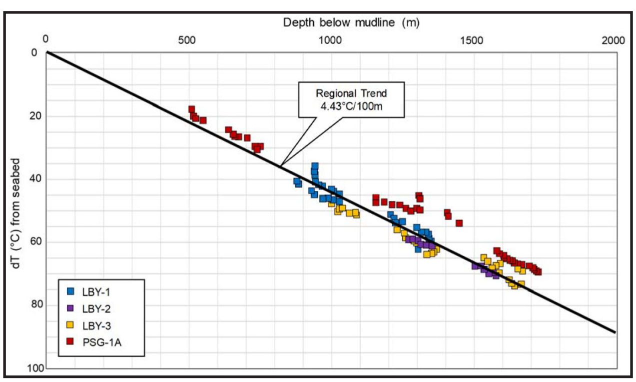

Figure 12: Average geothermal gradient from deep measurements of nearby wells, offshore Sabah.

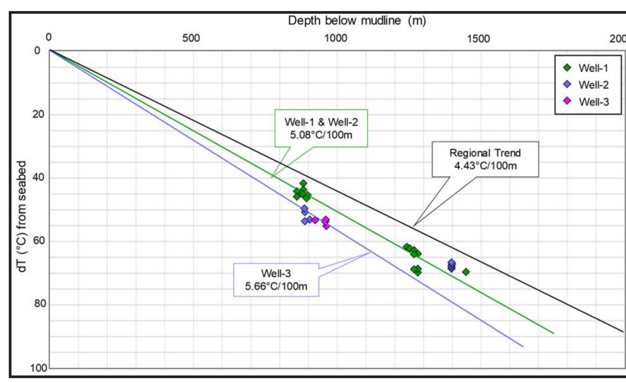

Figure 13: Average geothermal gradient from deep measurements of wells in Block X Study Area.

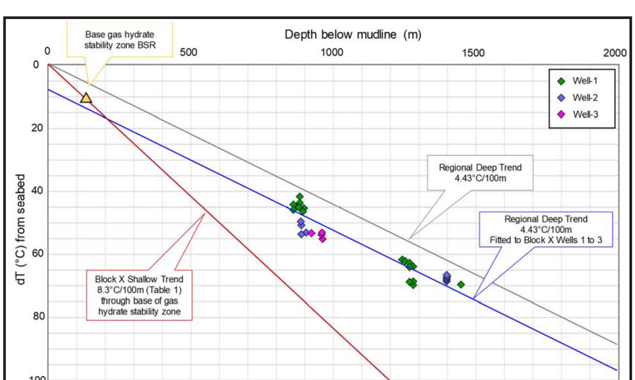

Figure 14: Regional deep trend fitted to Block X Study Area wells overlain by shallow trend.

the base of the gas hydrate stability zone. This gradient of 8.3°C/100m is consistent with the seabed gridded value (Jong *et al.*, 2013) (Figures 7 and 8). Importantly the regional trend of 4.43°C/100m (in blue) fits the data from all the Block X Study Area wells although it is noted that deriving a good linear fit from these sampling clusters is open to some interpretation.

A geothermal gradient function can be defined that is consistent with both the shallow seabed values and the deep data from the Block X Study Area wells by combining the two curves into a composite complex function (Figure 15). But are these complex composite curves both reasonable and consistent with the geological context of Block X and can they be successfully modelled?

Where a simple geothermal gradient is present the isotherms are evenly spaced with depth and the base of the gas hydrate stability zone is flat. A profile through this simple model (Figure 16, pink line) shows a uniform gradient that can be described by a simple linear function.

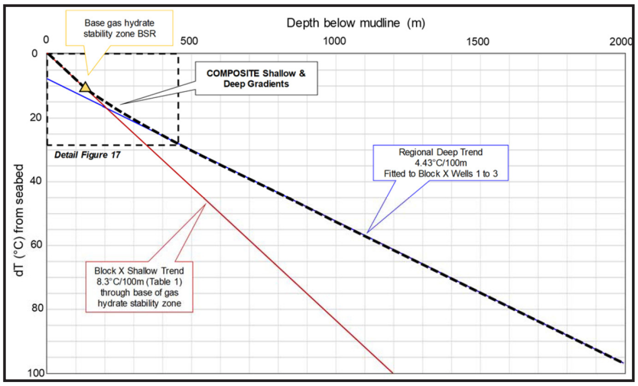

Figure 15: Composite geothermal gradient fitting all Block X Study Area data.

If a plume of warm fluids is introduced into the simple model the previously uniform isotherms become disturbed, rising above the plume in response to the additional heat input (Figure 16, central black profile). The isotherms become compressed increasing the geothermal gradient above the plume. A profile adjacent to the plume no longer gives a simple linear gradient but a complex curve reflecting the distortion due to the additional heat input. The base of the gas hydrate stability zone also rises and the geothermal gradient between the seabed and the base of the stability zone is significantly greater than the normal background gradient (Figure 16).

The validity of the model is tested in Figure 17. The lower panel presents the composite geothermal gradient model from Figure 16 rotated to the same orientation as previous Figures 12 to 15. The upper panel, extracted from Figure 15, shows the composite geothermal gradient curve fitted to all the data in the Block X Study Area. There is a close correlation between the two panels suggesting that

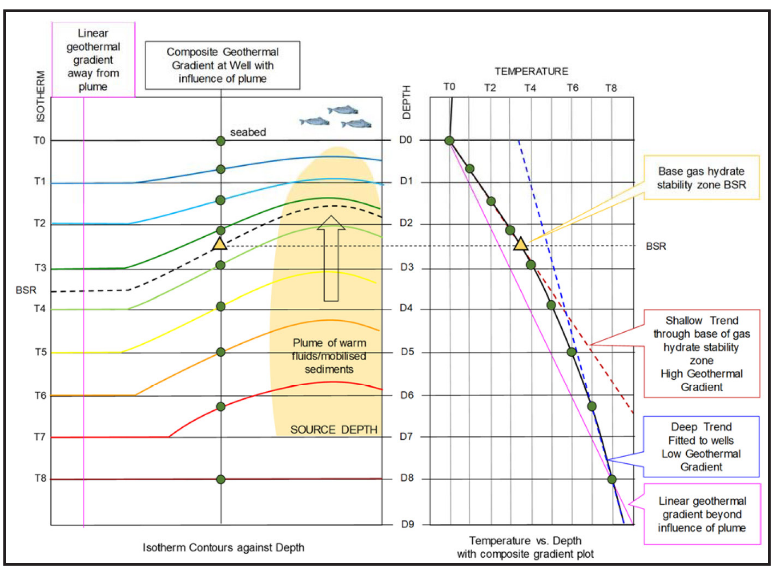

Figure 16: Composite Geothermal Gradient Model with influence of rising warm plume (schematic).

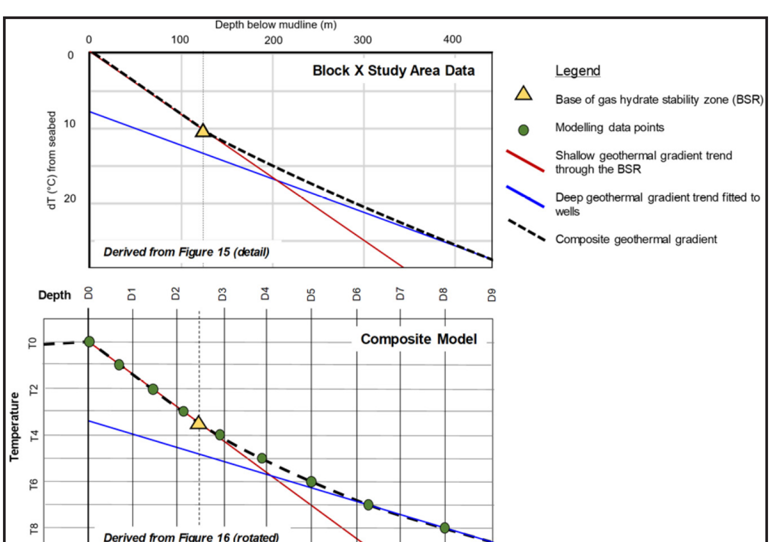

Figure 17: Comparison of Block X Study Area Data and the Composite Geothermal Gradient Model with influence of rising warm plume (schematic).

the heat input into the shallow section from rising plumes is responsible for the distortion in the geothermal gradients.

CONCLUSIONS

Geothermal gradients derived from seabed heat flow measurements and calculations from the position of the base of the gas hydrate stability zone consistently show a high to very high, variable geothermal gradients. It is interpreted that this is due to heat input into the shallow section from rising plumes of warm fluid and locally mobilised mud. In contrast, data from deeper sections within the Block X Study Area exploration wells have a lower gradient. Initial interpretation of these data show a geothermal gradient greater than the regional average but still significantly lower than the shallow values.

Reinterpretation of the Block X Study Area deep geothermal gradient well data suggests that the regional gradient fits these data if the influence of the warm fluid plumes on the shallow section is taken into account. The resultant gradient is no longer a simple linear function but a complex curve that will vary depending upon the offset of a well from the areas of anomalous warming in the shallow section.

A lower geothermal gradient at reservoir depth in the Block X Study Area, as suggested by this study, could have important implications for hydrocarbon maturation and generation. Hence, this observation would impact on the basin modelling outcomes such as the investigation conducted by Jong *et al*. (2014) in Block X, and warranted recalibration of geothermal functions to achieve more definitive modelling outcomes on timing of source rock maturation and hydrocarbon generation of the study area. In addition, a better understanding of heat flow data and modelling at target reservoir depths, in particular at potential well locations would play a paramount role in selection of well and logging equipment suitable for high temperature (and likely high pressure) drilling operations.

Last but not least, we believe similar heat flow measurements had been conducted by various operators with a few hot spots encountered in other actively explored deepwater acreages. Therefore, it would be useful if the heat flow database can be made available for comparison with this study to provide a better regional understanding of heat flow variations and their potential causes in the context of petroleum basin evolution in the greater area of deepwater Sabah.

ACKNOWLEDGEMENTS

We thank our exploration and drilling colleagues in JX Nippon for their technical support and discussion on presence of hydrates, mud volcanoes, hot plumes and interpretation of geothermal gradients based on seabed heat flow measurements and well data in the study area. These discussions have enriched the concept of more complex geothermal gradient functions in deepwater Sabah presented in this paper. Our gratitude is also extended to our reviewers Dr. Franz Kessler and Mr. Jim Fitton for their constructive comments that enhanced the quality of this paper.

REFERENCES

Anonymous JOIDES, 1992. Program for calculation of base gas hydrate stability. JOIDES Journal, 18, Special Issue No. 7.

Goh, H. S., Jong, J., McGiveron, S. & Fitton, J., 2017. A case study of gas hydrates in offshore NW Sabah, Malaysia: Implications as a shallow geohazard for exploration drilling and a potential future energy resource. National Geoscience Conference, 9-10 October 2017. Warta Geologi, 43(3), 205-207.

Grevemeyer, I. & Villinger, H., 2001. Gas hydrate stability and the assessment of heat flow through continental margins. Geophysics Journal International, 145, 647-660.

Hall, R., 2002. SE Asian Heatflow: call for new data, SE Asia Research Group, Department of Geology Royal Holloway University of London. http://searg.rhul.ac.uk/searg_uploads/2015/01/hf.pdf. Accessed 1 April 2018.

Hall, R. & Morley, C.K., 2004. Sundaland Basins. In: Continent-Ocean Interactions within East Asian Marginal Seas. Geophysical Monograph Series 149, American Geophysical Union.

Jong, J., Khamis, M.A. & Dasun, F., 2013. NW Borneo and Deepwater Block R (DWR) geothermal gradient and heat flow maps: An interpretation of DWR seabed heat flow measurement project and integration with regional database. JX Nippon Internal Document (unpublished).

Jong, J., Dayang Aimi Nuraini Awang Bakar and Mohd Asraf Khamis, 2014. Basin modelling study of Deepwater Block R (DWR) offshore Sabah and its correlation with surface geochemical analyses. Proceedings of International Petroleum Technology Conference, KLCC, December 10-12, DOI 10.2523/IPTC-18186-MS.

Kenyon, C.S. & L.R. Beddoes, 1977. Geothermal gradient map of Southeast Asia. South East Asia Petroleum Exploration Society and Indonesian Petroleum Association. 50 p.

Kvenvolden, K. A., 2000. Natural gas hydrate: introduction and history of discovery. In: Max, M.D. (Ed.), Natural Gas Hydrate in Oceanic and Permafrost Environments. Dordrecht Kluwer Academic Publishers, 9-16.

Laird, A.P. & Morley, C.K., 2011. Development of gas hydrates in a deepwater anticline based on attribute analysis from 3D seismic data. Geosphere, 7(1), 1-20. DOI: 10.1130/GES00598.1.

López, C. & Ojeda, G.O., 2006. Heat flow in the Colombian Caribbean from the Bottom Simulating Reflector. Cienca, Tecnología y Futuro, Vol. 3(2), Bucaramanga Jan./Dec. 2006.

McGiveron, S. & Jong, J., 2016. Morphological description of a mud volcano caldera from deepwater Sabah – general implications for hydrocarbon exploration. Warta Geologi, 42(3-4), 69-79.

Minshull, T.A., 2011. Some comments on the estimation of geothermal gradients from the depths of Bottom Simulating Reflectors. Proceedings of the 7th International Conference on Gas Hydrates (IGCH2011), Edinburgh July 17-21, 2011.

Ogawa, K. & Jong, J., 2016. A leaking hydrocarbon charge system in deepwater Sabah – Evidence from reservoir fluid geochemistry and mud gas isotope analysis. Proceedings of the 39th IPA Convention and Exhibition, Jakarta Convention Centre, May 25 -27, 2016.

Pollack, H.N., S. Hurter & J.R. Johnson, 1990. The new global heat flow data compilation. Eos Transactions American Geophysical Union, 71, 1604.

Pollack, H.N., S.J. Hurter & J.R. Johnson, 1993. Heat flow from the Earth's interior: analysis of the global data set. Reviews of Geophysics, 31, 267–280.

Rutherford, K.J. & M.K. Qureshi, 1981. Geothermal gradient map of Southeast Asia 2nd edition – 1981, South East Asia Petroleum Exploration Society and Indonesian Petroleum

Association. 51 p.

Searie, 2013. Measurement of marine crustal heat flow in the South China Sea. Report prepared for JX Nippon Oil & Gas Exploration (Deepwater Sabah) Limited, JX Nippon internal document (unpublished).

Shankar, U., Thakur, N.K. & Reddi, S.I., 2004. Estimation of geothermal gradients and heat flow from Bottom Simulating Reflector along the Kerala-Konkan basin of Western Continental Margin of India. Current Science, 87, 250-253.

Van Rensbergen, P. & Morley, C.K., 2001. Fluid expulsion from overpressured shale, an alternative for shale diapirism. Examples from offshore Brunei. Conference Proceedings, Subsurface Sediment Mobilisation Conference, University of Ghent, September 11-13 (abstract).

Zielinski. G.W., Bjorøy, M., Zielinski, R.L.B. & Ferriday, I.L., 2007. Heat flow and surface hydrocarbons on the Brunei continental margin. AAPG Bulletin, 91(7), 1053-1080.

Manuscript received 5 June 2018
Revised manuscript received 7 June 2018
Manuscript accepted 8 June 2018